43. TECTONIC SYNTHESIS, LEG 66: TRANSECT AND VICINITY[1]

Joel S. Watkins,[2] Kenneth J. McMillen,[2] Steven B. Bachman,[3] Thomas H. Shipley,[4]
J. Casey Moore,[5] and Charles Angevine[3]

ABSTRACT

Cores recovered from eight sites drilled along a transect across the Middle America Trench off southwestern Mexico show that accretion and offscraping of trench turbidites and the pelagic-hemipelagic blanket covering the ocean crust has been active for approximately 10 m.y. Active offscraping and imbricate underthrusting have been limited to the lower slope, whereas middle and upper slopes show uplift due to underplating by subducted sediments and younging of ocean crust. Offscraped trench sands of Pleistocene to Miocene age have been uplifted as much as 2 to 3 km above the present-day trench floor by combined accretion and underplating.

Sediment input into the subduction zone is partitioned, with roughly equal amounts being offscraped, underplated, and subducted. The offscraped component appears to consist primarily of trench turbidites, whereas the subducted component is thought to consist primarily of pelagic-hemipelagic sediments. The trench turbidite component probably dominates the underplated component.

Partitioning values based on mass balance budget and on theoretical lithospheric bending were comparable. This comparability lends confidence to our theory of flux partitioning.

Although we find no direct evidence of tectonic erosion, there is indirect evidence to support the feasibility of the mechanism, and although there is no present forearc basin, differential uplift rates suggest incipient development.

Thus we infer the following history of the region:

23-20 Ma—reorganization of plate motion: relative movement of Pacific and North American plate changes from oblique normal (subduction) to parallel (sinistral strike-slip) with margin subsidence and marine transgression.

19-17 Ma—margin sinks rapidly to, or just below, CCD, then begins slow rise. Sinistral strike-slip motion continues.

~10 m.y.—plate motion changes from strike-slip to normal-oblique; accretion begins and continues to present.

INTRODUCTION

The purpose of this chapter is to draw together data and inferences developed during seismic, sedimentological, and paleontological studies in the Leg 66 area and from these to develop an integrated interpretational picture of the tectonic evolution of the Leg 66 transect area. Principal elements of the paper are (1) the accretionary model of Seely et al. (1974); (2) the hypothesis of sediment subduction and subduction erosion of the underside of the overriding plate; (3) the underplating mechanism that may contribute to uplift of the margin and growth of the accretionary wedge; and (4) the geologic history of the margin during the 23-m.y. interval documented by cores.

Processes of mass addition or accretion discussed in this chapter have no standardized terminology. Thus we use "accretionary prism" or "accretionary wedge" to refer to all material that is structurally transferred from the lower to the upper plate during crustal convergence. "Offscraping" describes accretion (principally of trench sediments) at the base of the trench slope. "Underplating" designates a process of mass addition at depth beneath the rind of offscraped deposits. In our usage the term *accretion* refers to mass addition in general, whereas *offscraping* and *underplating* indicate a particular tectonic setting for the accretionary process. *Subduction erosion* refers to erosion of the underside of the accretionary wedge during subduction, whereas *tectonic erosion* encompasses subduction erosion and removal of material by strike-slip faulting.

Drilling results have been described at length in other chapters. The reader is referred especially to those by Lundberg and Moore, Shipley, and McMillen and Bachman for details of discussions summarized here. Figures 1, 2, 3, and 4 show the site locations and geology along the Leg 66 transect.

ACCRETION

The concept of accretion evolved during the late 1960's and early 1970's. Seyfert (1969) first pointed out that accretion-related deformation of trench sediments could explain the abrupt disappearance of seismic reflectors at the foot of the slope in seismic traverses across turbidite-filled trenches and inner trench walls. Dickinson (1971) suggested that although ocean basement is carried down with the descending lithosphere, lighter sediments are probably scraped off against the overriding plate and combine with ophiolitic scraps to form melanges. Dickinson further observed that the tectonic thickness of a melange zone depends on the amount of turbidite sediment fed into the subduction zone.

Von Huene (1972), using improved seismic reflection data, observed ocean crust and overlying undeformed pelagic sediments beneath deformed slope sediments ex-

[1] *Initial Reports of the Deep Sea Drilling Project*, Volume 66.
[2] Gulf Science and Technology Company, Pittsburgh, Pennsylvania.
[3] Department of Geological Sciences, Cornell University, Ithaca, New York.
[4] Scripps Institute of Oceanography, University of California, San Diego, La Jolla, California.
[5] Earth Sciences Board, University of California, Santa Cruz, Santa Cruz, California.

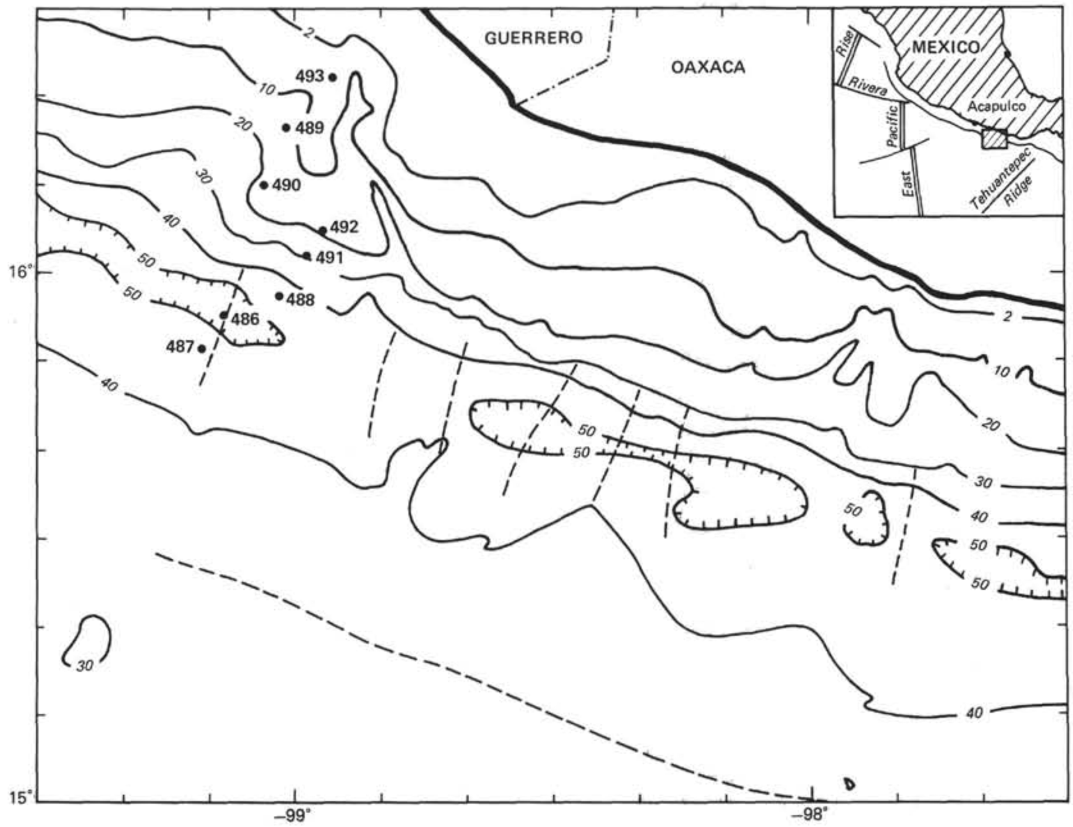

Figure 1. Index map of DSDP Leg 66 transect showing sites, bathymetry, and location of seismic data (dashed lines) used to estimate flux of trench turbidites and oceanic pelagites and hemipelagites being accreted and/or subducted. Contour interval is 100 meters. 5000-meter contours are approximate outlines of turbidite ponds in the trench.

tending up to 12 km landward of the Aleutian Trench. Although thrust faults were not clearly evident in the slope seismic data, von Huene's interpretation suggested their existence. He also made an estimate of the maximum amount of sediments accreted in the inner wall. Beck's (1972) multifold seismic section across the Java Trench near Bali showed undeformed ocean crust gently dipping beneath the inner wall for a distance of about 40 km landward of the trench. The region above ocean crust, though strongly hyperbolated with diffractions, suggested landward-dipping reflections.

Dickinson (1973) strengthened the argument for accretion with the observation that with few exceptions, widths of arc-trench gaps are proportional to ages of the respective island arc-trench systems. This resulted, he thought, from steady accretion of crustal materials by the inner wall.

DSDP Leg 31 drilled the toe of the slope landward of the Japan Trench off the island of Shikoku in mid-1973. Cores showed that Pleistocene trench sediments had been compressed to about half their original volume and given a distinct cleavage within 6 km of the trench. Elevation of these sediments to 300 meters above the trench floor (Karig et al., 1975) provided further evidence of accretion.

Seely et al. (1974) integrated the foregoing observations in their interpretation of multifold, common-depth-point seismic reflection data collected off Guatemala and Oregon, inferring that the inner wall was comprised of (1) a surficial apron of undeformed sediments overlying (2) a zone of deformation containing landward-dipping reflectors (LDRs), all overlying (3) relatively undeformed, gently landward-dipping oceanic crust. They suggested rotation of LDRs during accretion resulting in dip increase with elevation within the section. They interpreted this to mean that older, upper melange slices rotated upward as younger slices were progressively emplaced by underthrusting (Fig. 5).

Uplifted trench sands in the Leg 66 area suggest that the Seely et al. (1974) imbricate underthrust mechanism is active in the lower slope but not in the middle and upper slope region. Trench sands appear to have been uplifted at relatively rapid rates during offscraping at the toe of the slope, then uplifted at slower rates once incorporated within the slope. The increase in age of sands upslope is one of the strongest arguments for the offscraping model.

Although we did not penetrate thrust faults that we could biostratigraphically document, seismic data suggest penetration of a Pleistocene thrust fault in lower slope sediments at 488. Thrust faults are evident elsewhere in seismic data (Fig. 6). Failure to penetrate a demonstrable thrust fault was disappointing but not surprising in light of our discovery that drilled LDRs are associated with sand bodies and of the fact that we did not penetrate far below the slope sediment apron. The

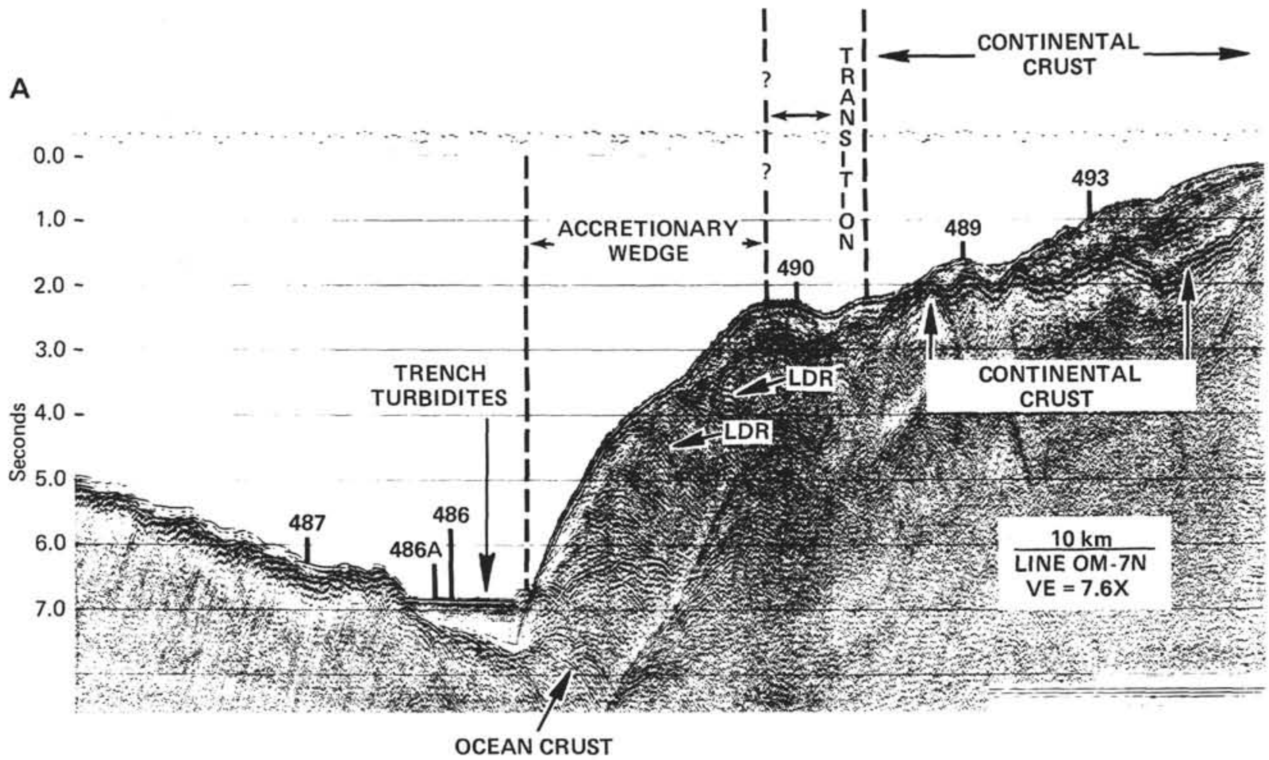

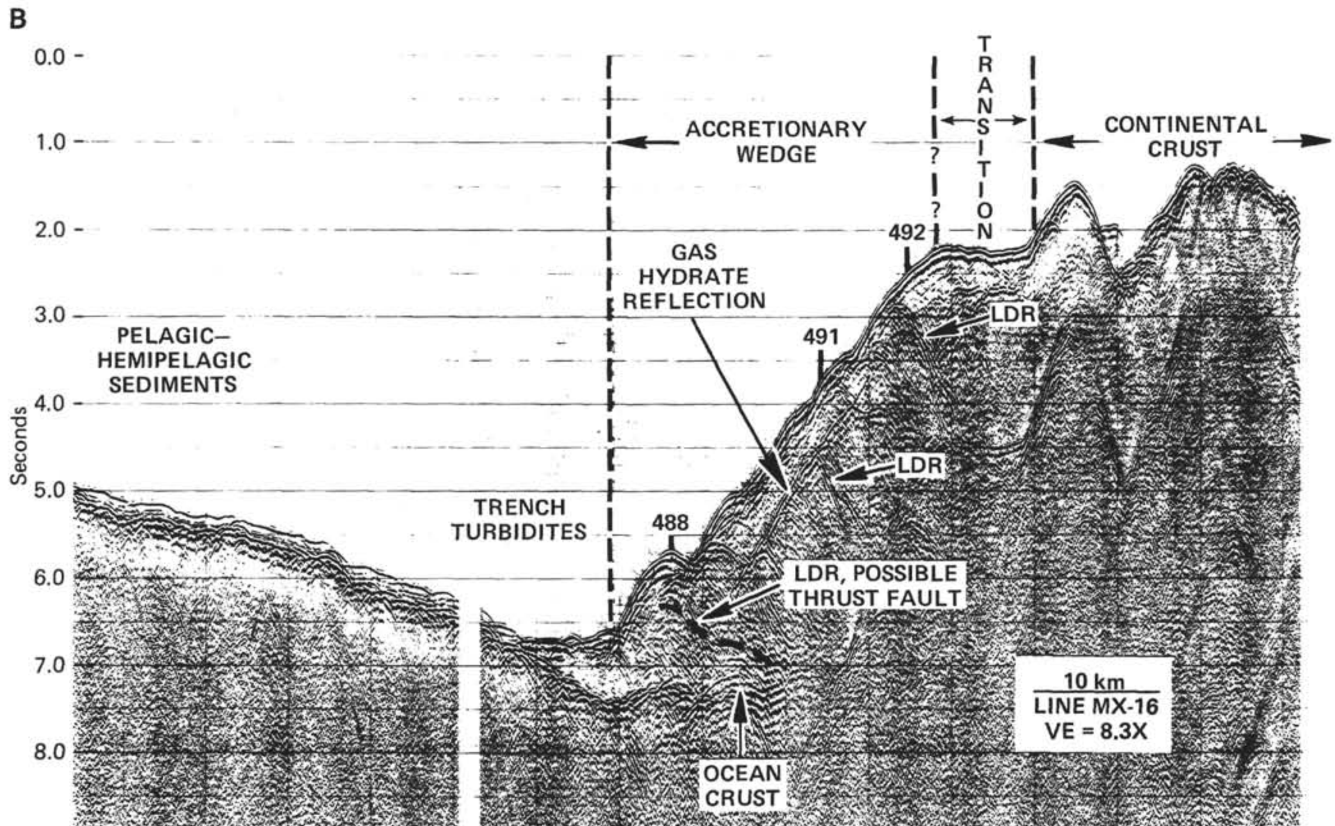

Figure 2. Seismic lines through Leg 66 sites (unmigrated time sections). A. UTMSI Line OM-7N through Sites 487, 486, 490, 489, and 493, showing major features (after Shipley et al., 1980). B. UTMSI Line MX-16 through Sites 488, 491, and 492, showing major seismic structures (after Shipley et al., 1980). The frontispiece of this volume is a composite of lines MX-16 and OM-7N displayed in color and in black and white.

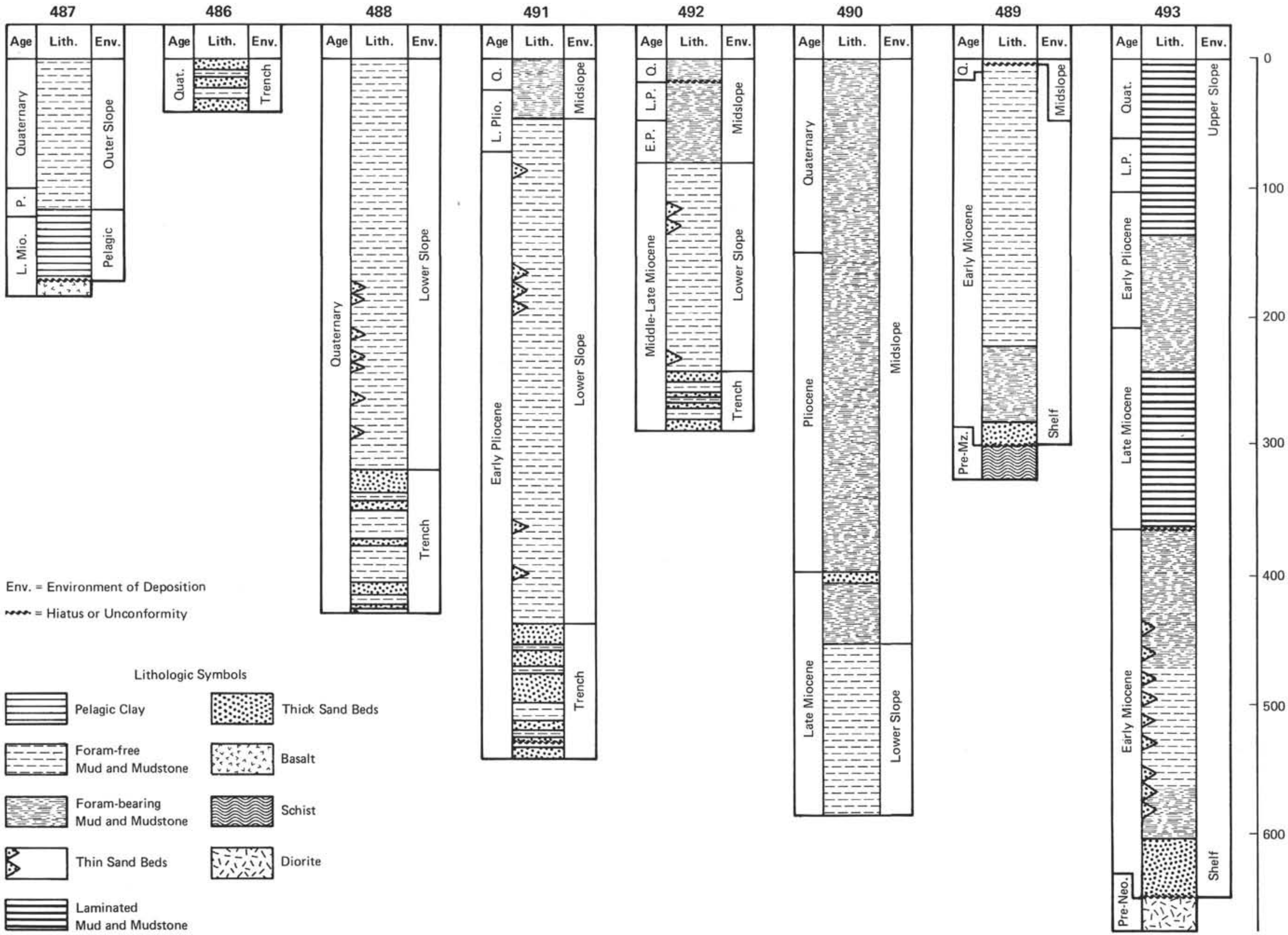

Figure 3. Stratigraphic columns showing results of Leg 66 drilling.

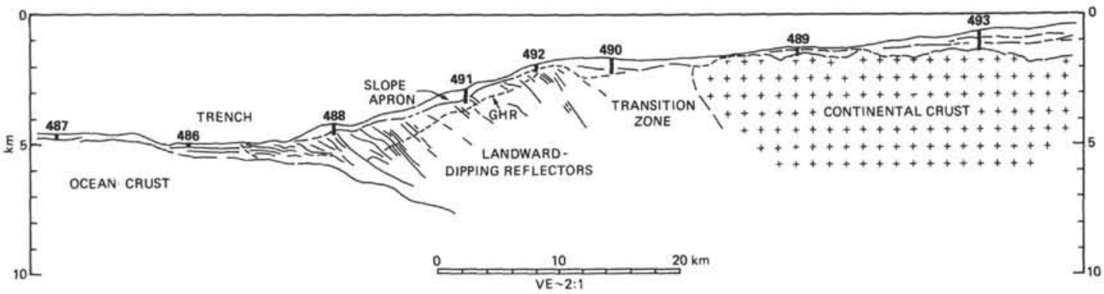

Figure 4. Composite structure cross section based on drilling results and migrated depth sections of UTMSI seismic lines OM-7N and MX-16 (Moore et al., 1979a). See frontispiece of this volume for analogous seismic time sections and color amplitude display.

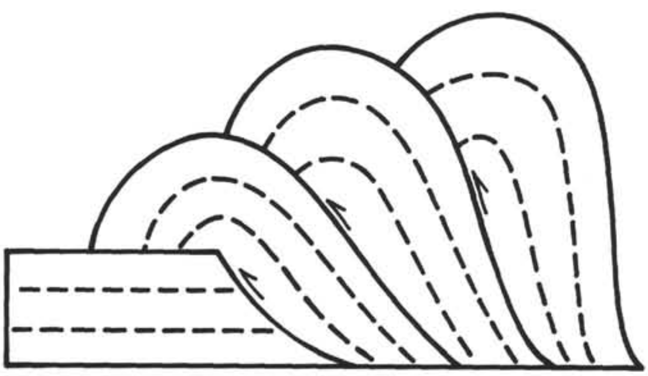

Figure 5. The imbricate underthrust accretionary model of Seely et al. (1974). Sediments (flat-lying segment to left) are progressively scraped off the underlying ocean crust and incorporated into the accretionary wedge to the right. Insertion of each new wedge into the bottom of the stack elevates and rotates overlying wedges with the result that major boundaries and internal stratigraphy (possibly LDRs) exhibit progressive steepening of dip upslope.

high sedimentation rates in the area require large fault offsets in order to verify biostratigraphically the existence of a fault.

Although our data indicate offscraping in the Leg 66 area, doubt remains regarding the universal applicability of the model. In their analysis of approximately 2000 km of multifold seismic reflection data collected by UTMSI, Shipley et al. (1980) observe that internal reflections are common in the western half of the Leg 66 area. They further infer that reflectors occurring in discrete zones are uplifted turbidites and that their occurrence in the western half of the zone is associated with the presence of a large submarine canyon and a turbidite pond in that part of the area. Shipley et al. (in press) examined Middle America Trench data from Mexico, Guatemala, and Costa Rica. Data from these areas support the idea that sandy turbidites greatly enhance offscraping. Much if not all ocean floor pelagic and hemipelagic sediments seems to be subducted.

Von Huene et al. (1980) drilled into the lower slope off Guatemala during Leg 67 and produced results strikingly different from those off southwest Mexico. In a hole 3 km landward of the trench, Leg 67 penetrated a Cretaceous to Pleistocene claystone and hemipelagic sequence before bottoming in mafic and intermediate igneous rock atypical of ocean basalts. Seismic data suggest several hundreds of meters of sedimentary rock between the bottom of the hole and ocean crust. Ladd et al. (1978) and Ibrahim et al. (1979) showed that seismic refraction and reflection interval velocities within the

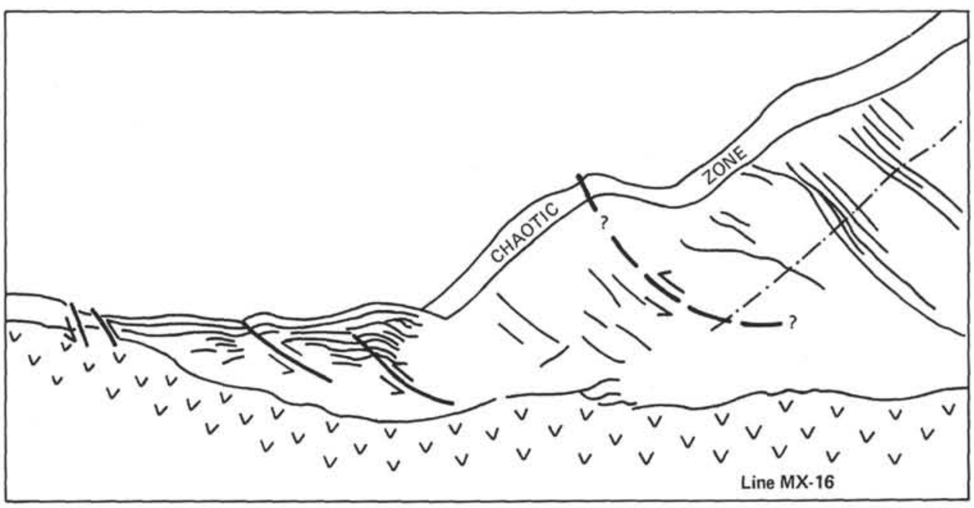

Figure 6. Line drawing of toe of slope from UTMSI migrated seismic Line MX-16, showing landward-dipping reflectors (LDRs) and inferred thrust faults (from Shipley et al., 1980).

main body of the Guatemala accretionary zone range from 4.1 to 6.5 km/s. Coring in the Leg 67 area produced relatively fresh mafic rock fragments. The site survey data suggested to J. W. Ladd (personal communication, 1978) the possibility of ophiolite slivers within the Guatemala slope.

Dickinson's (1973) observation that the width of arc-trench gaps (and, by inference, the volume of accretionary zones) are for the most part proportional to the age of the respective subduction zones suggests that accretion may also proceed by a mechanism other than offscraping of sandy turbidites such as observed at the Leg 66 site. One such mechanism is the accretion of slices of ocean crust, seamounts, or other crustal topographic irregularities. The sandy-turbidite and ocean-crustal-slice models may be end-members of a sequence with mature accretionary prisms and melanges, including examples of both.

SEDIMENT SUBDUCTION AND TECTONIC EROSION

Sediment Subduction

Mass Balance. The question of sediment subduction was recognized early by von Huene (1972), who estimated the volume of sediment accreted in the Aleutian subduction zone. Dickinson's (1973) observation of increasing trench-arc gaps, and by implication of increasing size of accretionary wedges with age, pointed at the problem. Karig and Sharman (1975) indicated the possibility of sediment subduction. Moore et al. (1979a, 1979b) and Shipley et al. (1980) suggested sediment subduction in the Leg 66 region, and von Huene et al. (1980) require it in the Leg 67 area.

The Leg 66 area offers a good opportunity for calculation of the amount of sediment being subducted. The current accretionary event began about 10 Ma. The relative youth of this system in comparison with many other subduction systems minimizes errors arising from changes in convergence rate and direction. Data from the East Pacific show the latest ridge jump and possible plate reorganization occurring about 10 to 15 Ma (Handschumacher, 1976; van Andel et al., 1975), before the onset of the current accretionary event. The plate system appears to have been stable thereafter.

Seismic velocities indicate that virtually the entire Leg 66 accretionary wedge consists of sediments. The velocities are sufficiently well defined to permit good estimates of the porosity and hence permit estimation of degree of partitioning of subducted fluids and rock.

Density of seismic data, both reflection (Shipley et al., 1980) and refraction (Shipley et al., 1980; Helsley et al., 1975; Mooney et al., 1975), are sufficient to define the geometry of the accretionary wedge, the trench turbidite wedge, and the thickness of the pelagic-hemipelagic ocean crust component.

The simplest procedure for calculating sediment subduction is as follows:

Input flux

1) Estimate thickness of sedmentary units (1) pelagic-hemipelagic component, (2) turbidite wedge component.

2) Calculate porosity from drill core (Shephard, this volume) and seismic velocities (see Eaton and Watkins, 1970).

3) Calculate equivalent input of nonporous rock.

4) Assume present-day convergence rate of 7 cm/y. (Minster and Jordan, 1978) applicable to last 10 m.y.

5) Calculate sediment input for 10 m.y.

Accretionary zone volume

1) Construct structure cross section from data of Shipley et al. (1980), Moore et al. (1979a, 1979b), Helsley et al. (1975), Mooney et al. (1975), and Keller et al. (1979) (Fig. 7).

2) Measure area of accretionary wedge.

3) Calculate equivalent nonporous rock vol./km of trench as Input flux steps (2) and (3).

Compare results

Thicknesses of pelagic-hemipelagic and turbidite-sand units vary locally. For trench turbidites they were averaged from data from seven seismic dip lines and for the pelagic-hemipelagic component (Fig. 2), along a 100-km seismic line 50 km seaward of and parallel to the trench. Results are as follows:

Unit	Thickness Min. (m)	Thickness Max. (m)	Thickness Avg. (m)	Velocity (km/s)	Porosity (est.) (%)	Rock Equiv. (m)
P-H	0[a]	200+	110	1.6	75[b]	30
TT	0[a]	625	260	1.8	40[c]	160
AZ	—	—	—	3.5	20[d]	—

Note: P-H = pelagic-hemipelagic, TT = trench turbidites, AZ = accretionary zone.
[a] Below limit of seismic resolution of about 25-50 m.
[b] From core measurements, Hole 487.
[c] Estimated from core recovered, Hole 486.
[d] Estimated from seismic velocities.

Clearly, trench turbidites (and associated downslope transported deposits) account for most of the sediment flux. It appears that a column equivalent to approximately 190 meters of nonporous rock has been feeding into the subduction zone at a rate of 7 cm/y. or 70 km/m.y. for the past 10 m.y.—which aggregates 135 km^3 per linear kilometer of trench.

We are aware that part of the input flux may be derived from slumping of accretionary zone sediments and thus does not represent new material. The lack of long hiatuses in lower slope holes and the minor extent of recognized slumps in the seismic data suggest, however, that sediment recycling is minimal relative to other input parameters. Furthermore, we have approached the measurement of input very conservatively in that we have ignored most slump material, some of which may be new material derived from slumping of the hemipelagic apron. We thus believe that if we have erred in our estimate of the slump flux component, the error probably results in too little flux rather than too much.

We now estimate the volume of the accretionary wedge. The principal uncertainty in the calculation is the size and shape of the landward part of the accretionary wedge triangle. Overhanging continental crust both obscures reflections from depth and introduces serious

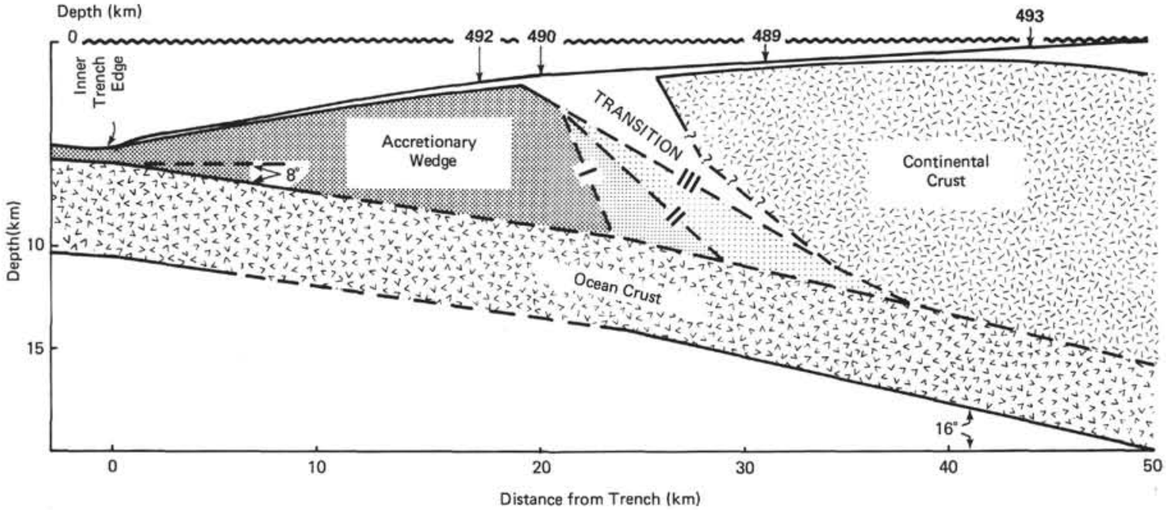

Figure 7. Hypothetical model used to estimate volume of the accretionary wedge. Base of crust near Site 493 and the trench is constrained by seismic refraction data (Helsley et al., 1975; Mooney et al., 1975). Top of the ocean crust beneath the trench and seaward part of the wedge is constrained by seismic reflection data (Shipley et al., 1980). Remaining features are inferred from a combination of Leg 66 drilling data and seismic reflection data (Shipley et al., 1980). I, II, and III represent minimal, probable, and maximum landward extent of the accretionary wedge, respectively.

errors in refraction calculations. Thus we project the Moho both landward and seaward, using refraction data from Helsley et al. (1975) and project ocean crust landward, using reflection data from Shipley et al. (1980) (Fig. 7). The undetermined upper landward surface of the accretionary zone, we divide into Cases I, II, and III, representing our estimate of minimum, probable, and maximum volumes of the accretionary wedge. Our "probable," Case II, results from projection landward of the landwardmost strong LDR, which we interpret as at or near the top of the accretionary wedge. Case IV includes the transition zone within the accretionary wedge (we consider this last case improbable).

The following summarizes results:

Case	Volume of Accretionary Zone (km^3/tkm[a])	Equivalent Volume of Nonporous Rock (km^3/tkm[a])	Amount Subducted (km^3/tkm[a])	(%)
I	97	77	58	43
II	111	89	46	34
III	135	108	27	20
IV	161	129	6	4

[a] tkm = linear kilometer of trench.

The foregoing gives a range of values derived from varying assumptions regarding the shape of the accretionary wedge. The value of sediment subduction we consider most likely is 34%. Percentages of subducted sediments in Cases I, II, and III range from 20 to 43%; exceed the pelagic-hemipelagic input, and require subduction of a significant fraction of trench deposits. This result supports the conclusion (Shipley et al., 1980) that most pelagic and hemipelagic sediments entering the Middle America Trench are being subducted. Our result is also consistent with Leg 67 data requiring subduction of a major portion of the pelagic-hemipelagic flux there (von Huene et al., 1980).

From a mechanical point of view, it is probably significant that the input sediment flux contains a water volume roughly equal to the volume of nonporous rock. Some water, especially in trench turbidites, is probably squeezed out during initial deformation, but seismic evidence of undeformed pelagic-hemipelagic layers extending to depths of several kilometers suggests that a considerable volume of water remains trapped within the sediments. The combination of the high clay and high water content in these sediments probably results in overpressuring and a low coefficient of friction, which provide a good decollement surface.

Pelagic-hemipelagic input thus appears preferentially subducted, whereas overlying sediment may or may not be scraped off and accreted. Scholl's and Marlow's (1974) observation that pelagic sediments are rare within melanges, as well as their absence in any of the three lower slope and one transition zone holes of Leg 66, supports preferential subduction of these sediments.

Flexural Loading. We also compared sediment flux calculations based on the observational model (Fig. 8) with calculations derived from a theoretical sediment loading model that calculates volumes of sediment accreted during a given time span from average uplift rates across the accretionary prism.

It is well known that the lithosphere will bend under loads. Using thin elastic plate theory, a number of authors have modeled the bending of lithosphere at ocean trenches (Gunn, 1937; Hanks, 1971; Watts and Talwani, 1974; Caldwell et al., 1976). Karig et al. (1976) used an elastic plate model to demonstrate that accretion at a trench creates a load capable of depressing the downgoing lithosphere. We followed these earlier models in assuming the lithosphere behaves as an elastic plate overlying an incompressible fluid. For thin plates

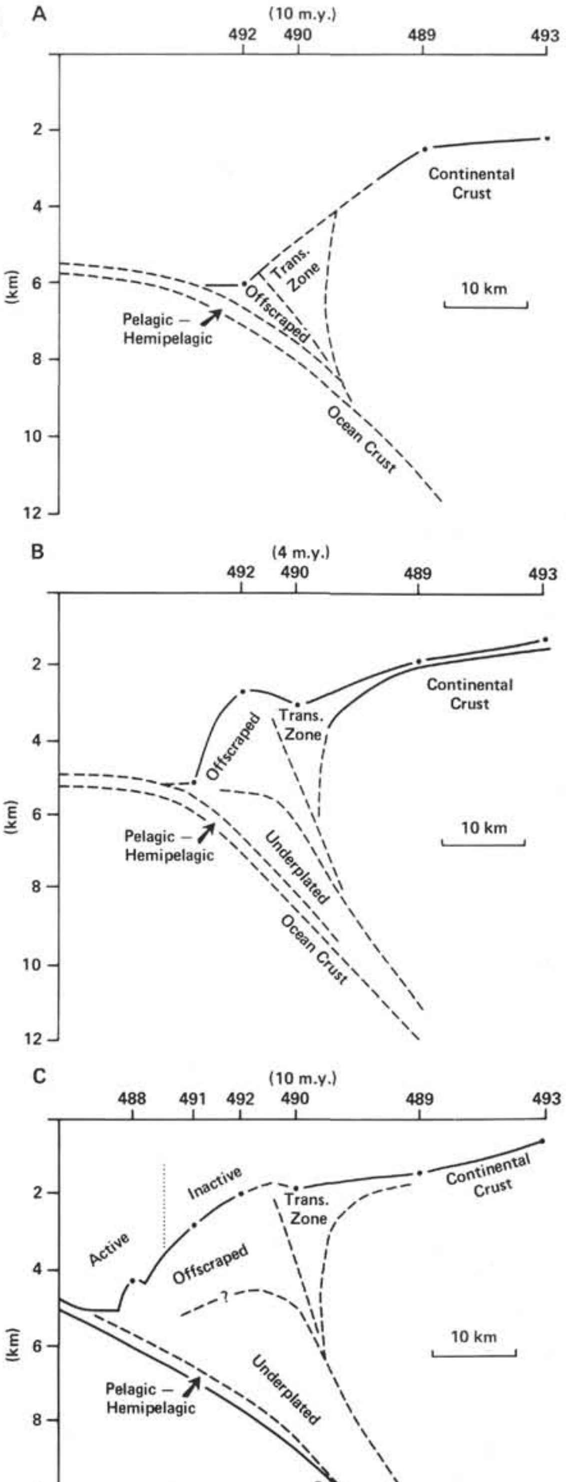

Figure 8. Hypothetical reconstruction of accretion-underplating sequence for Leg 66 transect, based on paleobathymetric data from Leg 66 sites. A. Onset of accretion, 10 Ma. "Transition zone" may consist of sediments deposited before onset of accretion or earliest accreted sediments. B. Early Pliocene, 4 Ma. Accretionary wedge is building seaward, underplating causes uplift of the continental crust, transition zone, and innermost accretionary wedge. C. Present. Underplating continues to elevate margin from Sites 491 to 493. Active accretion limited to vicinity of trench, Site 488.

and small deflections this theory is linear; the sum of the deflections due to a set of loads is equivalent to the deflection produced by the sum of the loads. With this principle we may break up the irregular load, represented by the accretionary prism, into a number of point loads.

The governing equation for two-dimensional flexure under a load $P(x)$ is

$$D \frac{d^4w}{dx^4} + kw = P(x), \qquad (1)$$

where D is the flexural rigidity, w is the vertical deflection, and k is a hydrostatic restoring force. In our problem, $k = (\varrho_m - \varrho_w)g$, where ϱ_m and ϱ_w are the densities of the underlying mantle and water, respectively, and g is the gravitational acceleration. We may solve (1) for a point load p at $x = 0$ (Hetenyi, 1946) as follows:

$$w = \frac{p\lambda}{2(\varrho_m - \varrho_w)g} e^{-\lambda x} [\cos\lambda x + \sin\lambda x], \qquad (2)$$

where $\lambda = (k/4D)^{1/4}$. In Figure 9 we show a point load of accreted sediment with density ϱ_s. The point load p is the mass of the submerged, accreted sediment multiplied by g and the physical dimensions of the column:

$$p = (\varrho_s - \varrho_w)\, gy\Delta x, \qquad (3)$$

y is the height of the column and Δx is the width. This column will cause a deflection w according to (2). The resulting topography at this location will be

$$t = y - w. \qquad (4)$$

Of course the other point loads which make up the accretionary prism will also cause deflections; these deflections must be subtracted from the right-hand side of (4) to obtain the bathymetry. The method for doing this involves convolving Equation (2) with all the point loads. For n point loads the topography at the ith point load will be

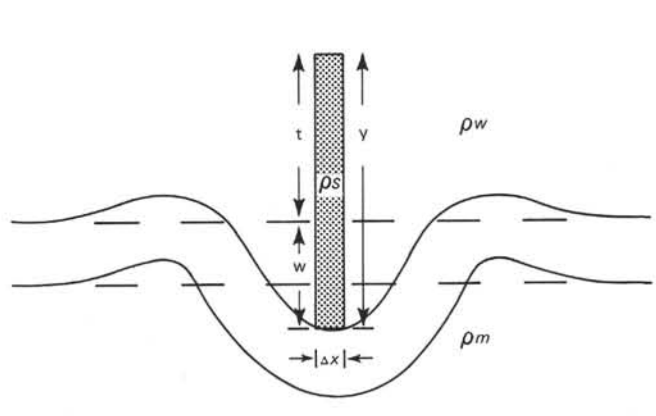

Figure 9. Deflection of the lithosphere under a point load of accreted sediment.

$$t_i = y_i - \sum_{j=0}^{n} K_{ji}K_j, \quad (5)$$

where $i = 0, 1, 2, \ldots, n$. The function K is known as the kernel of the equation and may be written

$$K_{ji} = \frac{\lambda(\varrho_s - \varrho_w)\Delta x}{2(\varrho_m - \varrho_w)} e^{-\lambda(j-i)\Delta x} [\cos\lambda (j - i)\Delta x + \sin\lambda (j - i)\Delta x]. \quad (6)$$

Equation (5) may be rewritten as

$$t_i = \sum_{j=0}^{n} (\delta_{ji} - K_{ji})\, y_j, \quad (7)$$

where δ_{ji} is the Kronecker delta (if $j = 1$, $\delta_{ji} = 1$; if $j \neq i$, $\delta_{ji} = 0$). Now Equation (7) is simply a matrix equation relating topography to thickness. Thus we may solve for y_j by inverting the matrix A with elements $A_{ji} = \delta_{ji} - K_{ji}$:

$$y_i = \sum_{i=0}^{n} A_{ij}{}^{-1} t_i \quad j = 0, 1, \ldots, n. \quad (8)$$

With this result we may calculate the total mass M needed to produce the topography

$$M = \sum_{j=0}^{n} \varrho_s y_i \Delta x. \quad (9)$$

The real power of this technique lies in the linearity of the governing Equation (1). If we know the change in topography of the accretionary prism during any period of time we may calculate the change in mass of the prism over the same period. The mass M will have two sources, accreted sediment and a smaller component due to trench slope deposits. Uplift rates determined from the DSDP coreholes show how the prism topography changes through time. The coreholes are 3 to 6 km apart—too far to use the point load equations; for this reason we linearly interpolated between wells to obtain more uplift rates. We used a spacing of $\Delta x = 1$ km.

These calculations present a problem: Caldwell and Turcotte (1979) showed that the flexural rigidity D of ocean lithosphere depends on its age. When the lithosphere is young and near the ridge axis it is very hot and consequently weak. As it grows older and cools, the lithosphere becomes more rigid. Over the last 5 m.y. the age of lithosphere being subducted in our study area has decreased from approximately 16 m.y. to 9 m.y. in age (Schilt et al., personal communication). We have used Caldwell's and Turcotte's (1979) Figure 3 to obtain the proper values of flexural rigidity.

It is well known that ocean lithosphere sinks as it ages and cools. Davis and Lister (1974) determined the subsidence rate $dw/d\tau$ to be

$$\frac{dw}{d\tau} = 164\,(\tau)^{-1/2}, \quad (10)$$

where the subsidence rate is expressed in m/m.y. and τ is m.y. The age of lithosphere entering the trench gets older with time, t ($t = 0$ at present time), as

$$\tau = \tau_o + \frac{V_c - V_r}{V_r} t, \quad (11)$$

where τ_o is the age of lithosphere presently being subducted, V_c is the convergence rate, and V_r is the spreading half rate. If we let $\tau_o = 6$ m.y., $V_c = 7$ cm/y., and $V_r = 3.5$ cm/y. (Schilt et al., in preparation), we determine an uplift rate dw/dt for the accretionary prism of

$$\frac{dw}{dt} = \frac{dw}{d\tau}\frac{d\tau}{dt} = 328.0\,(6.0 + t)^{-1/2}, \quad (12)$$

where the uplift rate is in m/m.y. and time t is in m.y. Uplift rates calculated with this result are approximately 100 m/m.y. These uplift rates due to a progressively younger subducted plate must then be subtracted from the uplift rates calculated by McMillen and Bachman (this volume); the remainder is the uplift rate due to sediment offscraping/underplating.

Using the sediment loading model, the total amount of sediment offscraped and/or underplated within the accretionary prism (seaward of the leading edge of the continental plate) was calculated. To determine this volume of sediment, the sediment point loads calculated from the model were integrated over the width of the prism at 1-m.y. time intervals. This volume was then corrected to an equivalent volume of nonporous rock using an average porosity of 20% (Table 1).

To determine the ratio of sediment subducted to sediment accreted and/or underplated in the accretionary prism, the sediment input into the trench and trench slope was calculated by using a method similar to the one used for the observational model. A nonporous rock thickness of 30 meters of pelagic-hemipelagic deposits on the incoming ocean plate and 160 meters of

Table 1. Volumes of sediment added to accretionary prism from uplift rate/isostasy calculations are compared to input volumes from pelagic, trench turbidite, and slope sources. Comparisons of equivalent nonporous rock volumes suggest the percentage of input sediment subducted (or underplated) below the leading edge of the continental crust.

	Added to Prism		Sediment Input (Equivalent Nonporous)				
	Volume	Equivalent Nonporous	Pelagic +	Turbidite +	Slope =	Total	% Subducted
0–1 my	7.9	6.3	2.1	11.2	2.1	15.4	59
0–2 my	12.4	9.9	4.2	22.4	2.9	29.5	66
0–3 my	19.4	15.5	6.3	33.6	3.5	43.4	64
0–4 my	23.3	18.6	8.4	44.8	4.7	57.9	68
0–5 my	26.6	21.3	10.5	56.0	5.8	72.3	71
	km³/tkm[a]			km³/tkm[a]			

[a] tkm = linear kilometer of trench.

trench turbidites fed into the subduction zone at a rate of 7 cm/y. yields a probable average rate of sediment input from the ocean side. In addition, the amount of trench slope sedimentation can be determined directly from drill cores that penetrated these slope sediments. Equivalent nonporous rock volumes for the slope sediments were then calculated using porosities determined from physical properties studies (Shephard, this volume). The relative importance of pelagic, trench turbidite, and slope deposition is summarized in Table 1.

The volume of sediment input into the trench and trench slope exceeds the volume of accreted/underplated material needed to account for the uplift rate calculated from the cores. Indeed, the volume of pelagic and slope deposits alone accounts for 63% to 77% of the sediment volume added to the accretionary prism using this model. When average trench turbidite fill is included, 59% to 71% of the volume of sediment input must be transported landward of the leading edge of the continental crust. (Note that this fraction is only approximately equivalent to that derived from the model in Fig. 8. Calculations based on the Fig. 8 model assume a sloping accretionary wedge/continental crust interface dipping landward beneath the continental margin edge; sediment flexural model calculations assume a vertical boundary at the edge of the margin.) This sediment may then be underplated beneath the continental crust and/or subducted to deeper depths. Because of potentially complex responses from isostasy in this region, we have not included uplift rates from upper slope cores drilled above the leading edge of the continental crust.

The results from the sediment loading model indicate a somewhat larger volume of subducted sediments than the Figure 8 model. The models employ different assumptions and calculation methods, yet both indicate subduction of a significant volume of sediments.

Subduction Erosion

Not all old trench systems have wide arc–trench gaps; some appear to have anomalously small accretionary wedges for their inferred ages. Did these systems ever have larger wedges? If so, where are they now? And if they never had wedges, what is the reason for their absence? Subduction erosion has been suggested as the answer.

Hussong et al. (1976) examined what is perhaps the best-known example, in the Peru-Chile Trench, between 8° and 12°S latitude. Here, volcanic studies on land show evidence of subduction as old as mid-Mesozoic. Multifold seismic reflection and detailed seismic refraction studies however, suggest a narrow (~10 km) accretionary wedge comprised of low-velocity material (2.0–3.5 km/s) currently being uplifted. Immediately landward, the lower slope consists of a low-velocity apron of undeformed sediments underlain by rocks with velocities of 5 km/s, which are more consistent with those of continental meta-igneous rocks than with deformed trench turbidites. Hussong and others also find evidence of normal faulting within the 5 km/s zone. They interpret these data as indicating that not only are sediments being subducted but that the subduction process is eroding the leading edge and underside of the continental crust and subducting continental crustal fragments.

The Mexican margin in the Leg 66 area resembles the Peru-Chile margin in some respects. Land studies suggest that lower Tertiary and Cretaceous volcanic arcs lay much closer to the trench than does the present volcanic axis. As in the case of the Peru-Chile Trench, seismic reflection data suggest an anomalously small accretionary wedge, considering the probable age of the subduction. Seismic evidence of tectonic erosion, however, is less extensive in the Leg 66 region than in the Peru-Chile Trench.

Although Leg 66 drilling provided no direct evidence of subduction erosion, there is abundant evidence of subduction of sediments to suggest that subduction erosion of the margin is mechanically plausible. Margin subsidence recorded at Sites 489 and 493 is consistent with thinning of the crust, and it is not implausible that a period of subduction erosion preceded the onset of accretion.

UNDERPLATING

Folding, dewatering, fracturing, and thrusting in the Leg 66 area occurs early in the accretionary process. After this initial period of deformation, the accretionary wedge rises slowly, at roughly the same rate as the upper slope. The vertical distance between the accreted turbidites and the downgoing ocean crust is widening with time. The Seely et al. mechanism (1974) proposed uplift by rotation of imbricate wedges. Because this mechanism appears to be inoperative in the Leg 66 area except near the foot of the slope, there must be another explanation for uplift of the middle and upper slope. We believe underplating to be the operative mechanism (Fig. 8).

If the underplating model is correct, then the upper part of the accretionary wedge consists of trench turbidites and slope sediments. Judging from the thickness of actively offscraping material in the toe of the accretionary wedge (e.g., Fig. 6), we estimate the thickness of the offscraped crust to be about 2 km and its volume to be 60 to 65 km^3/tkm. Velocities of 3 km/s measured in this upper zone suggest an average porosity of 30%, and an equivalent nonporous rock volume of 45 km^3/per linear km, or 33% of the 10-m.y. input flux. This implies subduction of one-third of the input sediment flux beyond the zone defined by the accretionary prism in Figure 7. Thus about 33% of the total is being scraped off to form a rigid "crust" of the accretionary prism, another 33% is initially subducted then progressively "skimmed off" and underplated on the accretionary prism, and the remaining 33% is carried to greater depths. Since there is no reason to differentiate between underplating of the accretionary prism and underplating of the continental crust, it is simpler to divide our margin into (1) an accreted, rigid crust, (2) an underlying zone of underplating, and (3) a lowermost subduction zone of pelagites and hemipelagites. Figure 8 shows the inferred evolution of the Leg 66 transect.

Absence of a forearc basin in one of the more prominent anomalies of the Leg 66 area. There is some evidence, however, that an incipient forearc basin may be forming in the vicinity of Site 490. Paleobathymetric reconstruction (Fig. 10) indicates that the region between Sites 490 and 492 region is rising faster than between Sites 489 and 490. Further, seismic reflections in the slope apron near 490 are tilted landward, similar to those of the Iquique Basin (Seely, 1979). Persistence of differences in uplift rates observed in the region of Sites 489-490-492 will result in development of a forearc basin. A higher rate of underplating close to the trench may be the mechanism responsible for this pattern of uplift. Such a mechanism would cause the zone of maximum uplift to move seaward with time. Tectonic, thermal, and isostatic subsidence dominate in the landward portion (Karig and Sharman, 1975). Seaward migration of the trench-slope break as observed in Iquique Basin (Seely, 1979) is a predictable consequence of underplating, and forearc basins would widen with time as proposed by Karig (1974).

The relatively shallow depths of Sites 489 and 493 as well as isostatic effect of the continental crust probably limit the depth of any forearc basin developing in the Leg 66 area. One can visualize, however, a much deeper forearc basin developing in an area of ocean/ocean convergence.

TECTONIC HISTORY

The history of the margin in the Leg 66 area is interwoven with the history of the Pacific Plate, the Cocos Plate, and perhaps the Rivera and Caribbean plates as well. Evidence for plate motions is confusing and sometimes contradictory. Consequently, the history of the Leg 66 sites is not clear, especially during the period from 25 to 10 Ma. Sites 493 and 489 suggest the following history for the continental crust portion of the transect:

22 Ma—subsidence and marine transgression.

19 Ma—subsidence below CCD.

<19 Ma—gradual, uniform uplift to present position.

Lower slope Site 488, 491, and 492 indicate the following for the accretionary wedge portion of the transect:

10 Ma—earliest observed accretion.

<10 Ma—progressive accretion and seaward expansion of the accretionary wedge.

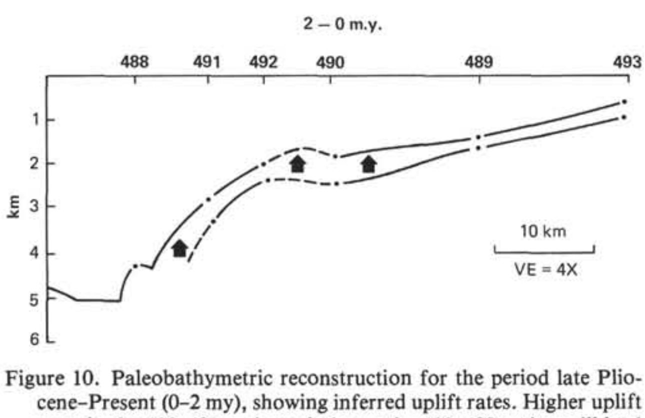

Figure 10. Paleobathymetric reconstruction for the period late Pliocene–Present (0–2 my), showing inferred uplift rates. Higher uplift rates in the 490–492 region relative to the 490–489 region will lead to the formation of a forearc basin if continued.

Inclusion of transition zone sediment in the accretionary wedge would push the onset of accretion back to 12 to 13 Ma. Absence of LDRs in the transition zone as well as atypical evolution evidenced by transition zone sediments, however, suggest that sediments in this zone were not emplaced by offscraping as at Sites 492, 491, and 488.

The data suggest that truncation and faulting away (probably strike-slip, according to Karig et al., 1978, and Malfait and Dinkleman, 1972) of a piece of the former continental margin occurred during a major plate reorganization, placed by Handschumacher (1976) between 26 and 20 Ma. Clabaugh and McDowell (1976) infer cessation of subduction 23 Ma, indicated by termination of volcanic activity in the Sierra Madre Occidental. Subsidence and marine transgression in the Leg 66 area suggest that this occurred no later than 22 Ma. Thus the data are in good general agreement regarding the time of the reorganization.

It is not clear, however, whether the ancient slope and shelf slipped dextrally northwest as part of the San Andreas development (Atwater, 1970), as suggested by Karig et al. (1978), or sinistrally to the southeast as suggested by several other investigators (e.g., Malfait and Dinkleman, 1972). The best evidence on this dilemma may be that reconstruction of Cayman Fracture Zone slippage of 2 to 4 cm/y. (MacDonald and Holcomb, 1978) places the Guatemala-Honduras corner of the Caribbean Plate near the Leg 66 area 12.5 to 25 Ma, or during the time of plate reorganization suggested by Pacific magnetic anomalies and in the time gap between end of subsidence and onset of accretion. Central American rocks south of the Motagua-Polochic faults, which separate the Caribbean and North American plates, contain granodiorite intrusives of Cretaceous and Tertiary ages (Seely, 1979; Fig. 8). We have no information indicating genetic affinities of these and Leg 66 intrusives, however. The evidence, although not compelling, favors sinistral strike-slip motion.

The lack of evidence of accretion during the interval between 22 and 10 Ma may indicate that motion was largely strike-slip during this interval, ending with the breakup of the East Pacific Rise south of the Baja California at 10 Ma (Handschumacher, 1976). Magnetic anomalies, however, are indistinct and interpretation ambiguous.

Site 490 may overlie sediments shed during the 22–10 m.y. interval. A deep penetration hole here might be rewarding in terms of the history of the Mexican margin and Pacific Plate motion reconstruction.

SUMMARY AND CONCLUSIONS

We drilled eight sites along a transect of the Middle America Trench off southwestern Mexico to investigate accretion and consumption of sediments and rock during the subduction process and to investigate the history of a young subduction zone.

Samples collected indicate that accretion has been active in the area for 10 m.y. or perhaps slightly longer. We recovered trench sands ranging in age from Pleistocene to Miocene and uplifted as much as 2 to 3 km above the present-day trench floor, and we observed progressive younging of offscraped and accreted trench sands downslope as predicted by the accretionary model. Landward-dipping reflectors considered to represent thrust faults in other areas were found here to be associated with uplifted trench turbidite sand sequences.

Uplifted sediments record an early period of deformation and uplift. In this period, which lasted 2 to 4 m.y. in our samples, sediment uplift rates were 600–800 m.y. Following this initial episode, most deformation ceases and uplift rates fall to 100 to 200 Ma.

Of sediment entering the subduction zone, 33% (mainly trench turbidites) is offscraped at the toe of the slope; 33% is initially subducted but then underplates the previously offscraped sediments, causing inner slope to rise with time; and 33% (probably including all the pelagite–hemipelagite oceanic component) is subducted landward beneath the continental crust. Trench turbidites and slumps account for 85% of the equivalent nonporous rock subduction flux, and the oceanic component accounts for 15%. Similar results from calculations based on the elastic response of the ocean crust bending under the weight of the accreting/offscraped sediments support our conclusion that a significant fraction of the sediment input is being subducted. Porosities of 75% in the pelagite–hemipelagite component result in large quantities of water being subducted. The water probably causes overpressuring and plays a major role in the lubrication of the suture.

We find no direct evidence of subduction erosion, but it seems reasonable to conclude that such erosion is mechanically feasible in view of the large quantities of sediment being subducted.

The absence of a forearc basin in the area of investigation is probably due to the youth of the subduction regime. The Sites 492 to 490 region is currently rising faster than the 490 to 489 region; continuation of this pattern of relative uplift could result in formation of a forearc basin.

The history of the region, documented by sediment cores and interpreted in light of the history of the neighboring plates, is as follows:

~23 Ma—reorganization of the Pacific Plate; cessation of volcanism in the Sierra Madre Occidental; volcanic axis subsequently shifts east; sinistral strike-slip faulting and removal of old margin. Marine transgression in Leg 66 area 22 Ma followed by rapid subsidence.

19–17 Ma—margin sinks to or just below CCD, begins slow rise.

~10 Ma—Baja California rift forms; change from strike-slip motion to oblique convergence. Accretion begins and continues to present.

REFERENCES

Atwater, T., 1970. Implication of plate tectonics for the Cenozoic tectonic evolution of western North America. *Geol. Soc. Bull.*, 81:3513–3536.

Beck, R. H., 1972. The oceans, the new frontier in exploration. *APEA J.*, 12 (Pt. 2):5–28.

Caldwell, J. G., Haxby, W. F., Karig, D. E., et al., 1976. On the applicability of a universal elastic trench profile. *Earth Planet. Sci. Lett.*, 31:239–246.

Caldwell, J. G., and Turcotte, D. L., 1979. Dependence of the thickness of the elastic oceanic lithosphere on age. *J. Geophys. Res.*, 84:7572–7576.

Clabaugh, S. E., and McDowell, F. W., 1976. Volcanismo Cretácico-Cenozoico y su relación con la evolución tectónica del occidente de México. *III Congr. Latinom. Geol., Resumes*, p. 35.

Davis, E. E., and Lister, C. R. B., 1974. Fundamentals of ridge crest topography. *Earth Planet. Sci. Lett.*, 21:405–413.

Dickinson, W. R., 1971. Plate tectonics in geologic history. *Science*, 174:107–113.

________, 1973. Widths of modern arc-trench gaps proportional to past duration of igneous activity in associated magmetic arcs. *J. Geophys. Res.*, 78:3376–3389.

Eaton, G. P., and Watkins, J. S., 1970. The use of seismic refraction and gravity methods in hydrogeological investigations. *In* Morley, L. W. (Ed.), *Mining and Groundwater Geophysics: Econ. Geol. Rep. (Geol. Surv. Can.)*, 26:544–568.

Gunn, R., 1937. A quantitative study of mountain building on an unsymmetrical earth. *J. Franklin Inst.*, 224:19–53.

Handschumacher, D. W., 1976. Post-Eocene plate tectonics in the eastern Pacific. *In* Sutton, G. H., Manghnani, M. H., and Moberly, R. (Eds.), *The Geophysics of the Pacific Ocean Basin and Its Margins: Am. Geophys. Union Monogr.*, 19:177–202.

Hanks, T. C., 1971. The Kuril Trench–Hokkaido rise system: Large shallow earthquakes and simple models of deformation. *Geophys. J. Roy. Astr. Soc.*, 23:173–189.

Helsley, C. E., Nation, J. B., and Meyer, R. P., 1975. Seismic refraction observations in Southern Mexico. *Am. Geophys. Union Trans.*, 56:452.

Hetenyi, M., 1946. *Beams on Elastic Foundation:* Ann Arbor (University of Michigan Press), pp. 1–26.

Hussong, D. M., Edwards, P. B., Johnson, S. H., et al., 1976. Crustal structure of the Peru-Chile Trench: 8°–12°S latitude. *In* Sutton, C. H., Manghnani, M. H., and Moberly, R. (Eds.), *The Geophysics of the Pacific Ocean Basin and Its Margin: Am. Geophys. Union Monogr.*, 19:71–86.

Ibrahim, A. K., Latham, G. V., and Ladd, J., 1979. Seismic refraction and reflection measurements in the Middle America Trench offshore Guatemala. *J. Geophys. Res.*, 84:5643–5649.

Karig, D. E., 1974. Tectonic erosion of trenches. *Earth Planet. Sci. Lett.*, 21:209–212.

Karig, D. E., Caldwell, R. K., Moore, G. F., et al., 1978. Late Cenozoic subduction and continental margin truncation along the northern Middle America Trench. *Geol. Soc. Am. Bull.*, 89: 265–276.

Karig, D. E., Caldwell, J. G., and Parmentier, E. M., 1976. Effects of accretion on the geometry of the descending lithosphere. *J. Geophys. Res.*, 81:6281–6291.

Karig, D. E., Ingle, J. C., Jr., et al., 1975. *Init. Repts. DSDP*, 31: Washington (U.S. Govt. Printing Office).

Karig, D. E., and Sharman, G. F. III, 1975. Subduction and accretion in trenches. *Geol. Soc. Am. Bull.*, 86:377–389.

Keller, B., Lewis, B. T. R., Meeder, C., et al., 1979. Exploration seismology studies of active and passive continental margins. *In* Watkins, J. S., Montadert, L., and Dickinson, P. W. (Eds.), *Geological and Geophysical Investigations of Continental Margins: Am. Assoc. Petrol. Geol. Mem.* 29:443–451.

Ladd, J. W., Ibrahim, A. K., McMillen, K. J., et al., 1978. Tectonics of the Middle America Trench. *Int. Symp. Guatemala Earthquake and Reconstruction Process*, Vol. 1.

MacDonald, K. C., and Holcomb, T. L., 1978. Inversion of magmatic anomalies and seafloor spreading in the Cayman Trough. *Earth Planet. Sci. Lett.*, 40:407–414.

Malfait, B. T., and Dinkleman, M. G., 1972. Circum-Caribbean tectonic and igneous activity and the evolution of the Caribbean plate. *Geol. Soc. Am. Bull.*, 83:251–272.

Minster, J. B., and Jordan, T. H., 1978. Present-day plate motions. *J. Geophys. Res.*, 83:5331–5354.

Mooney, W. M., Meyer, R. P., Helsley, C. E., et al., 1975. Refracted waves across a leading edge: Observations of Pacific shots in southern Mexico. *Am. Geophys. Union Trans.*, 56:452.

Moore, J. C., Watkins, J. S., Bachman, S. B., et al., 1979a. Middle America Trench Drilled. *Geotimes*, 24:22–22.

________, 1979b. Progressive accretion in the Middle America Trench, Southern Mexico. *Nature*, 281:638–642.

Scholl, D. W., and Marlow, M. S., 1974. Sedimentary sequences in modern Pacific trenches and the deformed circum-Pacific engeosyncline. *In* Dott, R. H., and Shaner, R. H. (Eds.), *Modern and Ancient Geosynclinal Sedimentation: Spec. Publ. Soc. Econ. Paleontol. Mineral.*, 19:193–211.

Seely, D. R., 1979. The evolution of structural highs bordering major forearc basins. *In* Watkins, J. S., Montadert, L., and Dickinson, P. W. (Eds.), *Geological and Geophysical Investigation of Continental Margin: Am. Assoc. Petrol. Geol. Mem.* 29:245–260.

Seely, D. R., Vail, P. R., and Walton, G. G., 1974. Trench slope model. *In* Burk, C. A., and Drake, C. L. (Eds.), *The Geology of Continental Margins:* New York (Springer-Verlag), pp. 249–260.

Seyfert, C. K., 1969. Undeformed sediments in oceanic trenches with seafloor spreading. *Nature*, 222:70.

Shipley, T. H., Ladd, J. W., Buffur, R. T., in press. Comparison of structural styles along the Middle America Trench—Mexico, Guatemala and Costa Rica. *In* Leggett, J. K. (Ed.), *Trench and Forearc Sedimentation and Tectonics in Modern and Ancient Subduction Zones:* London (Geological Society of London).

Shipley, T. H., McMillen, K. J., Watkins, J. S., et al., 1980. Continental margin and lower slope structures of the Middle America Trench near Acapulco (Mexico). *Mar. Geol.*, 35:65–82.

van Andel, Tj. H., Heath, G. R., and Moore, T. C. Jr., 1975. Cenozoic history and paleo-oceanography of the central equatorial Pacific Ocean. *Geol. Soc. Am. Mem.*, 143:134.

von Huene, R., 1972. Structure of the continental margin and tectonism at the eastern Aleutian trench. *Geol. Soc. Am. Bull.*, 83: 3613–3626.

von Huene, R., Aubouin, J., and Azema, J., 1980. Leg 67: The Deep Sea Drilling Project Mid-America Trench transect off Guatemala. *Geol. Soc. Am. Bull.*, 91:421–432.

Watts, A. B., and Talwani, M., 1974. Gravity anomalies seaward of deep-sea trenches and their tectonic implications. *Geophys. J. R. Astron. Soc.*, 36:57–90.